Boosting the performance of under-frequency load shedding by assessing the frequency-stability margin

Urban RUDEZ, Rajne ILIEVSKA, Denis SODIN, Rafael MIHALIC

University of Ljubljana, Faculty of Electrical Engineering

Slovenia

Contact person:
Urban RUDEZ
University of Ljubljana, Faculty of Electrical Engineering
Trzaska 25, 1000 Ljubljana, Slovenia
urban.rudez@fe.uni-lj.si
00386-1-4768-418
00386-41-756-735

Keywords:
under-frequency load shedding, power-system frequency stability, Rate-of-Change-of-Frequency, frequency-stability margin, active-power balance.

Abstract:
The modern electrical power systems are suffering from a decreasing trend in synchronously-connected rotational masses provided by the conventional power plants. Not only that; the volatility of weather conditions causes the effective rotational masses to be very stochastic. Such conditions require flexible and adaptable protection functions. However, under-frequency load shedding protection is still pursuing a decades-old single-criterion philosophy in majority of cases around the world. This is why in this paper, we suggest to boost the performance of under-frequency load shedding by upgrading the relay settings to depend on two criteria, rather than a single one. The new criterion is based on calculating the newly-defined time-dependent variable referred to as the frequency-stability margin. In order to calculate it, one has to have access to the frequency and its rate of change within the frequency relay. A non-complex filtering function proved to be sufficient for the concept to work extremely well in the laboratory environment that involved hardware-in-the-loop testing of a physical protection relay. The innovation opens up numerous further research possibilities that are either currently under investigations or will be in the near future.

1 Introduction

In the last couple of years, the quantity of synchronously-connected rotating masses in several electric power systems (EPS) suffers a falling trend with much higher volatility as before. At the same time, the number of frequency-related events in EPSs is increasing ([1], [2], [3]). Such outcome was expected due to the obvious correlation between both. Yet the under-frequency load shedding (UFLS) protection failed to keep the pace of technology transition that took place in the electricity-generating sector. Namely, it is a fact that up until recently UFLS was rarely activated, mainly because in the past EPS was over-dimensioned and built very robustly. New changing trends on the other hand are imposed extremely fast and this is why it is important to yield *feasible* UFLS upgrades to compensate for the lost time.

One can find several publications and initiatives for the research of frequency protection in 100%-converter interfaced generation (CIG) environment [4]. Having large interconnections in mind, this appears as exaggeration of what our society is aiming at, since sustainable development is based on harvesting renewable energy sources [5] that includes both hydro as well as nuclear power. One ought to keep in mind that both successfully and efficiently employ synchronous machine technology for decades and are not expected to do otherwise in the future. This is why it is much more reasonable to expect that both generating technologies (i.e. synchronous machines and CIG) will coexist for quite some time in the future, especially in large interconnections such as European continental interconnection ENTSO-E. This is why it appears reasonable to concentrate on solutions that considers the presence of both technologies and to assume that the stability of the electrical voltage frequency will keep playing an important role in bulk EPS operation.

By existing definitions, the only objective of under-frequency load shedding (UFLS) is to "*prevent a further frequency drop*" [6] or with other words "*restore the balance*" [7] between generated and consumed active power in the EPS in due time, i.e. before the frequency declines below the frequency-stability limit. In the available literature however, several other criteria can be found for the evaluation of UFLS operation as well (post-disturbance steady-state frequency, minimization of disconnected load, etc.), even though cited regulations clearly do not define them. Authors strongly believe that tasks of individual protection and control mechanisms should be clearly defined in order for them to function properly despite EPS complexity. This is why we consider it reasonable to draw a clear distinction between frequency-control and frequency-protection (i.e.) UFLS objectives. The prerequisite for achieving this is a flexible UFLS that efficiently balances generation and consumption in *any* operating condition. After automated UFLS halts the frequency decline as it is supposed to, it is a task of the frequency control (either conventional or fast frequency control brought by CIG units) to bring the frequency back to nominal value. We believe it is unacceptable to expect that one mechanism (e.g. frequency control) should be forced to handle negative consequences of inappropriate intervention of another (e.g. UFLS). This is exactly what is expected from frequency control in cases when conventional UFLS disconnects too much or too little loads in the EPS. Therefore, existing (conventional) UFLS has to be made more adaptable and flexible. At the same time, the efficiency level should not be diminished by bringing wide-area communication system (e.g. Wide-Area Monitoring System - WAMS) into the picture.

It is a common agreement, that Rate-of-Change-of-Frequency (*RoCoF*) is a most obvious candidate for enabling the required level of UFLS flexibility. On the other hand, algorithms implementing *RoCoF* usually invoke some scepticism, especially considering its calculation/estimation and filtering. Until now, researchers failed to figure out a transparent methodology for creating an universal *RoCoF*-based criterion within individual under-frequency relays. One can find several suggestions applying *RoCoF* in the context of wide-area solutions ([8], [9]), however, system operators in general are not keen on conditioning their system integrity protection schemes (SIPS) of such importance to a less reliable communication technology. In addition, these solutions are often dependent on the estimate of the EPS inertia, which is a complex problem by its own. The conservatism of protection engineers will probably always support local solutions rather than wide-area ones. This is why in this paper, we present the basics and the latest findings of a patent-pending solution (application no. PCT/EP2018/059048) of implementing locally measured *RoCoF* for the purpose of UFLS. It brings a required level of adaptability to UFLS, which was tested with hardware-in-the-loop (HIL) approach with real-time digital simulator (RTDS) at the University of Ljubljana in Slovenia.

The paper is structured as follows. In section 2 the technology main principles are outlined, beginning with the definition of a frequency-stability margin in section 2.1. The *f-M* plane is defined in section 2.2 and a supplemental relay tripping criterion is described in section 2.3. Simulation results are provided in section 3, separately for RMS (section 3.1) and EMT (section 3.2) mode of calculation. Finally, the conclusions are drawn in section 4.

2 Technology outline

The basic idea of the suggested technology goes back to 2011, when the authors published a scientific paper facilitating short-term frequency prediction in real time [10] for the first time. It was intended for use with WAMS, whose task was to gather and aggregate frequency measurements from several parts of the EPS. This is in fact the ground base for numerous research papers in this area, even nowadays. Namely, multiple authors consider the global EPS frequency known and available in the national control centre in real time. This is not so problematic when dealing with moderate or slow frequency changes. However, due to time delays introduced by Phasor Measurement Units (PMUs) and WAMS [4], [5], such solutions seem inappropriate for dealing with fast frequency changes.

In [10], the algorithm for a short-term frequency prediction was therefore run continuously and supported by WAMS. The only condition for its proper functioning was that the frequency measurements correspond to Center of Inertia (COI). In contrast to other publications, instead of relying on a swing equation for the estimation of the surplus/deficit amount of active power, the method continuously monitored the frequency predictions. Once it was recognized that the expected frequency will no longer violate the frequency-stability limit, UFLS was halted.

The algorithm in [10] and its improved successors [13], [14] were all considered as a smart supplement to locally executed conventional UFLS. However, in the following subsections, we will present the latest stage of

development that we believe has the potential to replace the conventional UFLS and is expected to operate efficiently in the actual EPS implementations.

2.1 Real-time calculation of a frequency-stability margin

State of the art Intelligent Electronic Devices (IED) that are usually implemented for performing UFLS activities can facilitate measuring electrical voltage frequency $f(t)$ and its rate-of-change $RoCoF(t)$ in real time. Since IEDs already perform conventional UFLS functionalities in terms of generating a trip signal once the frequency violates a pre-defined threshold [15], in this paper we do not discuss the problems of the frequency measurement process. We will however, provide some discussion on $RoCoF(t)$ calculation in section 3.

For the purposes of this subsection, let us assume both $f(t)$ and $RoCoF(t)$ are available in IED in each point in time. In addition, let us assume that a stabile EPS operation is disturbed by a large active-power incident causing a significant frequency decline as depicted in Fig. 1. EPS frequency stability is assessed by calculating a so-called frequency-stability margin $M(t)$, which we define as the expected time before the frequency is about to reach the frequency-stability limit f_{LIM} if the decay rate remains unchanged and equal to $RoCoF(t)$. Of course, it is expected that in reality the frequency will improve due to several control mechanisms, but it is extremely difficult to estimate how much. What matters is that we are aware of the fact that $M(t)$ calculation is a worst-case estimate of a frequency trajectory a couple of seconds in advance. Even at the first glance it is clear that $M(t)$ calculation requires solving a simple algebraic expression and is therefore not a subject to comprehensive computational efforts in the IED.

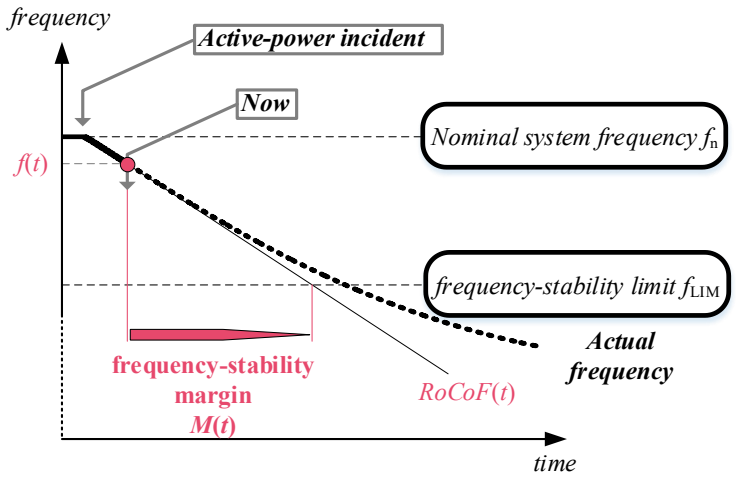

Fig. 1: Frequency-stability margin definition

In the next stage, let us explain what information can be obtained by $M(t)$. In Fig. 2, we depicted four different conditions. From *RoCoF*'s point of view, a pair of conditions 1/2 and 3/4 are identical. On the other hand, a pair of conditions 1/3 and 2/4 are identical from the perspective of frequency *f*. Nevertheless, by observing corresponding values of $M(t)$ in four different colours below the main graph it becomes clear that we are in fact dealing with four different conditions which cannot be determined as such unless we combine both $f(t)$ and $RoCoF(t)$ into a new variable. So we recognize that large values of $M(t)$ indicate less critical situations compared to small values of $M(t)$, regardless of whether these conditions originate from frequency already being low or $RoCoF(t)$ being large.

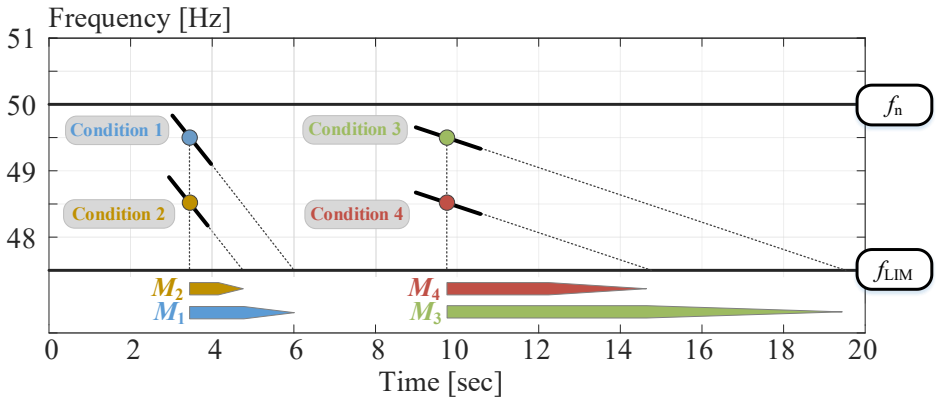

Fig. 2: Frequency-stability margin information

2.2 The definition of *f-M* plane

Once a frequency stability margin $M(t)$ is available, we suggest to introduce a new type of diagram in order to preserve the transparency of the situation despite dealing with an additional variable. This new diagram is referred to as the *f-M plane* in which an operating point follows different trajectories in different conditions. But let us first observe typical EPS frequency responses with respect to time after active-power incident takes place (see the upper graph in Fig. 3). Numerous curves correspond to different power-imbalance values. A red curve clearly depicts an extremely fast frequency decline that causes a violation of f_{LIM} soon after an incident. On the other hand, green curve corresponds to a small power-imbalance, which can be handled by the frequency control alone without the UFLS activation. Black curve depicts a borderline case in which f_{LIM} is not violated, yet the activation of conventional UFLS is still expected since several UFLS frequency thresholds are violated (please note that UFLS activation was not a part of this simulation).

A lower graph in Fig. 3 depicts the same set of conditions in a frequency $f(t)$ versus-frequency stability margin $M(t)$ plane, which we address as *f-M* plane. Prior to an incident, we are dealing with a nominal EPS frequency and $RoCoF = 0$. In the *f-M* plane, this corresponds to the location of the operating point far on the right-hand side of the diagram (see "*Pre-incident location*" notion). Once the incident occurs, *RoCoF* suddenly changes and at the same time, frequency is kept at nominal value. In the *f-M* plane, this corresponds to a sudden relocation of an operating point towards the left-hand side of the diagram. Of course, the actual value of the *RoCoF* determines how far to the left the operating point is relocated (see "*Moment of incident location*" notion). The most severe case (red) reaches farthest to the left compared to others. Lesser the *RoCoF* value, shortest the reach (green and black curves). In continuation (as the process of the actual frequency decline evolves), the operating point follows one of several possible trajectories. The trajectory is either *i*) redirected back towards the right-hand side of the diagram (green and black curves) or *ii*) diverted towards the diagram origin corresponding to $f = f_{LIM}$ and $M = 0$. By comparing both diagrams in Fig. 3 it is straightforward to conclude that only in cases, which violate f_{LIM}, the operating point comes into the vicinity of the diagram origin. At this point, it is important to recognize the similarity between the *f-M* plane and the impedance characteristic of the distance protection relay. Namely, this is the basis for the suggested modifications of frequency relays setting, presented in section 2.3.

2.3 Supplemental relay tripping criterion

Conventional UFLS is triggered according to a single criterion: violation of some pre-defined frequency thresholds f_{thr}. What we suggest is to update this with a supplemental criterion, based on the value of $M(t)$: the so-called frequency-stability margin threshold M_{thr}. Only when both criteria (i.e. $f(t) < f_{thr}$ and $M(t) < M_{thr}$) are satisfied at the same time, UFLS is initiated. In the *f-M* plane, this can be graphically represented as an *L*-shaped tripping characteristic. In Fig. 4 (left) one can observe the characteristics of six consecutive UFLS stages.

There are several advantages of the combined shedding criterion in Fig. 4 (left), which will be shown in section 3 by analysing actual dynamic simulations. However, to understand the entire scale of flexibility gained by this very simple supplement, it is best to draw reader's attention to the possible advanced parametrization of the tripping criteria in each frequency relay. For this purpose let us examine Fig. 4 (right) in which we show that it is possible to condition frequency-threshold settings f_{thr} with the value of $M(t)$. For small values of $M(t)$ it is usually reasonable to trip multiple stages simultaneously as soon as possible to halt the frequency decline as soon as possible. Therefore, certain stages can be scheduled for tripping at similar (or even equal) frequency thresholds –

see red notion in Fig. 4 (right). On the other hand, when the detected $M(t)$ is small and therefore the frequency declines gradually yet consistently, it is best to avoid tripping large portions of the load at the same time in order to avoid potential frequency overshoots. So increasing the shedding granularity by splitting the entire set of relays belonging to a certain UFLS stage into several sub-sets can significantly improve the process of power-rebalancing. Naturally, it is up to the system operator to decide whether advanced parametrization is reasonable for the specifics of the EPS under its jurisdiction or not. The simulation results in this paper do not include the advanced parametrization, since this segment of the technology is still under research.

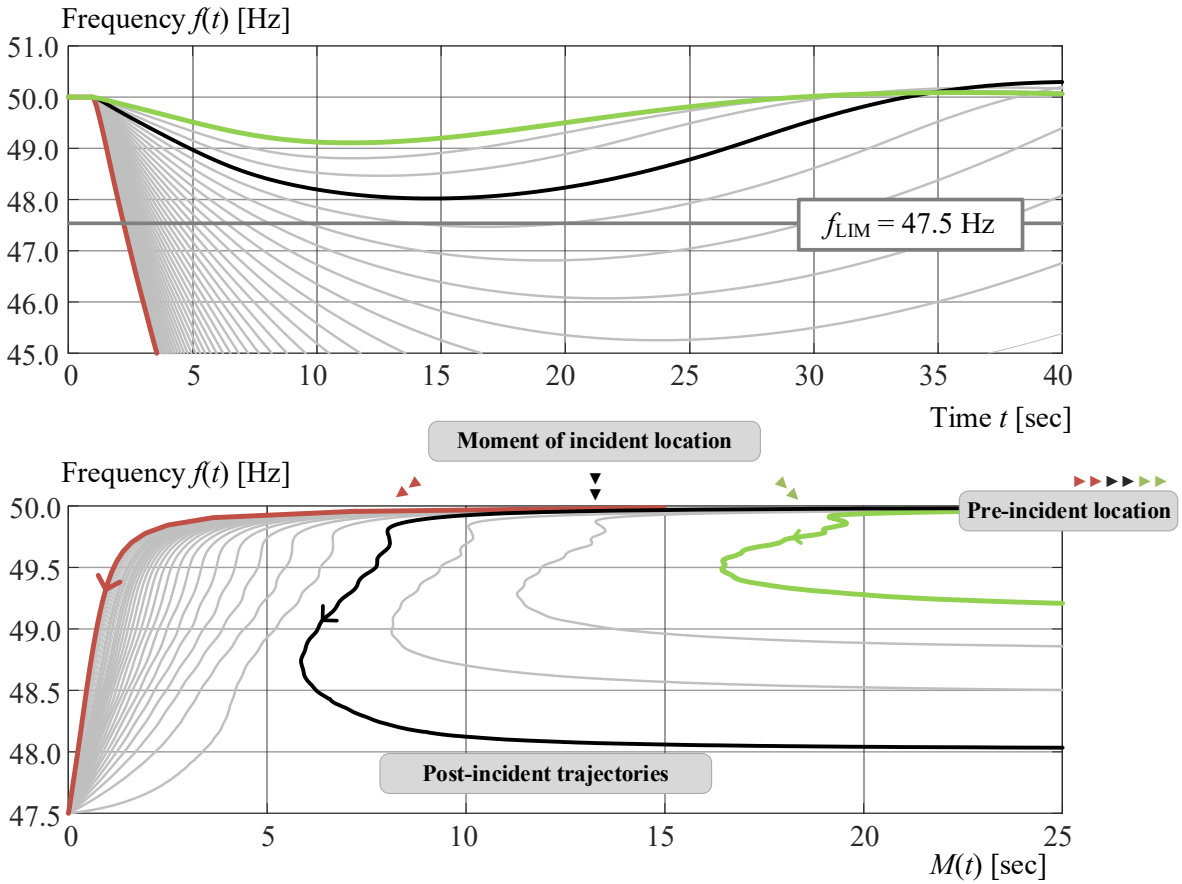

Fig. 3: The definition of an *f*-*M* plane

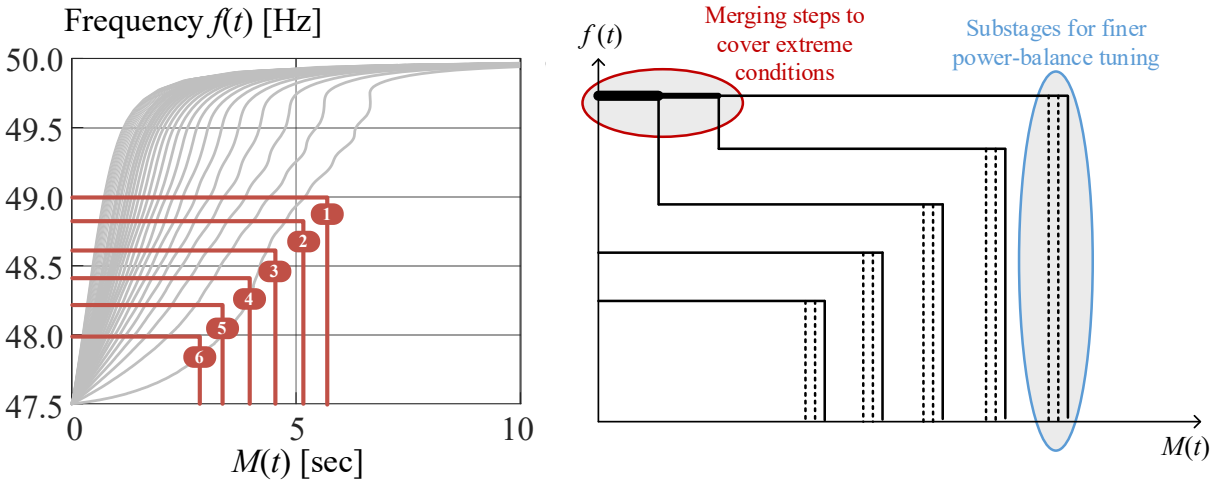

Fig. 4: Left: a combination of an existing (f_{thr}) and supplemental (M_{thr}) shedding criterion in *f*-*M* plane, right: advanced parametrization of the tripping criterion in each frequency relay

3 Simulation results

The presented approach was thoroughly tested by means of digital dynamic simulations using different commercially available simulation tools. The basic concept was developed and verified by running the off-line RMS dynamic simulations. The used dynamic model represented a portion of the Slovenian 110 kV network in which UFLS is activated several times per year. On the other hand, in order to increase the Technology Readiness Level (TRL), we additionally performed several tests with EMT dynamic simulation tool, which at the same time enables hardware-in-the-loop (HIL) tests, i.e. real-time digital simulator (RTDS). In RTDS, IEEE 9-bus test system was used for testing in which a physical relay controlled the loading on one of the system busses. The remaining loads were controlled by the digital replica of the relay functionality. Those applied the standardized frequency and *RoCoF* measurement procedures within RTDS, as programmed and validated by RTDS developers. Results confirm that despite dependent entirely on local measurements, described modification of conventional UFLS brings a high level of flexibility, adaptability and complete avoidance of over-shedding by fulfilling UFLS original objective. This makes the approach feasible for the actual implementation in real EPS applications.

3.1 Off-line RMS dynamic simulations

It is a known fact that by measuring the electrical voltage frequency $f(t)$, one is in fact trying to estimate the average speed of synchronous machines in the network. Frequency measurement and appropriate testing is therefore always a matter of discussion [16]. When it comes to *RoCoF*, things become even more debatable. Nevertheless, we believe that the results in this section confirm that our research provides a useful implementation of *RoCoF* for UFLS purposes, despite known *RoCoF* accuracy issues and noise involvement. In addition, the methodology has the potential for an impact in frequency control area as well. However, this is still a subject of research.

The most elementary concern that arises from the use of *RoCoF* is the time delay introduced by wide sliding windows required for *RoCoF* calculation. This is why we conducted some tests by varying a sliding window width from 50 ms up to 500 ms in RMS dynamic simulation. This was intended to show that newly introduced *RoCoF*-related time delays do not diminish the efficiency of UFLS. Fig. 5 depicts two cases: *i*) when initial *RoCoF* = -5 Hz/s (blue curves) and *ii*) when initial *RoCoF* = -0.5 Hz/s (red curves). It is clear from Fig. 5 that a sliding window width discussion is relevant only when fast-acting changes take place (blue curves). In addition, we see that once the frequency reaches 49.0 Hz threshold (this is usually the frequency value for the activation of the first UFLS stage) the variation of $M(t)$ is within a 0.5 seconds regardless of the selected window width. Since M_{thr} values are suggested to be in the range of a few seconds [17], the sliding window width clearly does not affect the triggering time of the initial UFLS stage. Namely, M_{thr} criterion is always fulfilled significantly above 49.5 Hz, which means that UFLS stage is activated at the same time as it would be in conventional UFLS (remember, frequency-related criterion is kept unaltered).

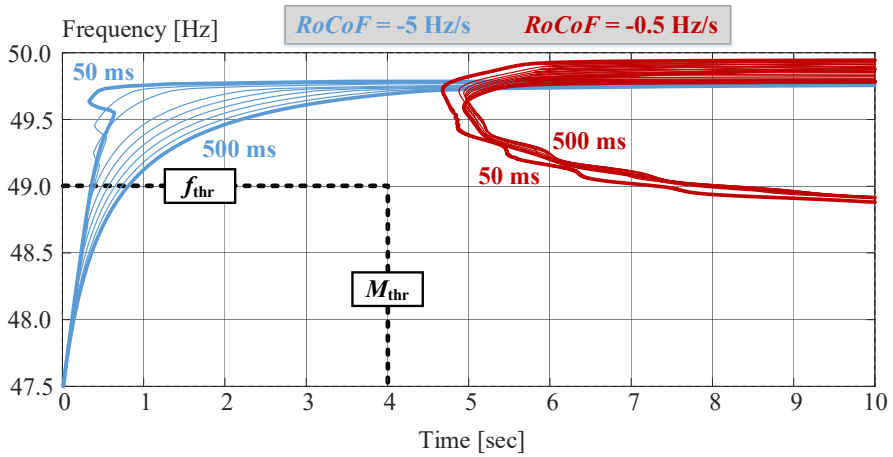

Fig. 5: The effect of a sliding window width required for *RoCoF* calculation

The main testing involved three sets of 60 cases (180 cases in total), each set having a different EPS inertia constant H = 3 sec / 6 sec / 9 sec). The differences between 60 cases within a single set is in the amount of

active-power imbalance after the incident. The results showed that by including a new tripping criterion, the frequency is allowed to drop lower in most cases, in average -0.42 Hz / -0.60 Hz / -0.68 Hz. On the other hand, 5 % of the system loading was kept supplied in all cases and overshoots are avoided in a great majority of cases. For reader's convenience, Fig. 6 depicts two actual simulation results out of those 180 cases. Dashed curves correspond to EPS frequency response using conventional UFLS approach, whereas solid curves indicate the improvement gained by adding a new *RoCoF*-based tripping criterion. As already written, a frequency drop below f_{thr} is allowed but only when f_{LIM} violation doesn't take place. In this way we make sure that UFLS protection does exactly what is was intended for, instead of poorly solving an under-frequency issue in such a way that it transforms it into an over-frequency issue. As known, the latter outcome is as much undesired at the former one.

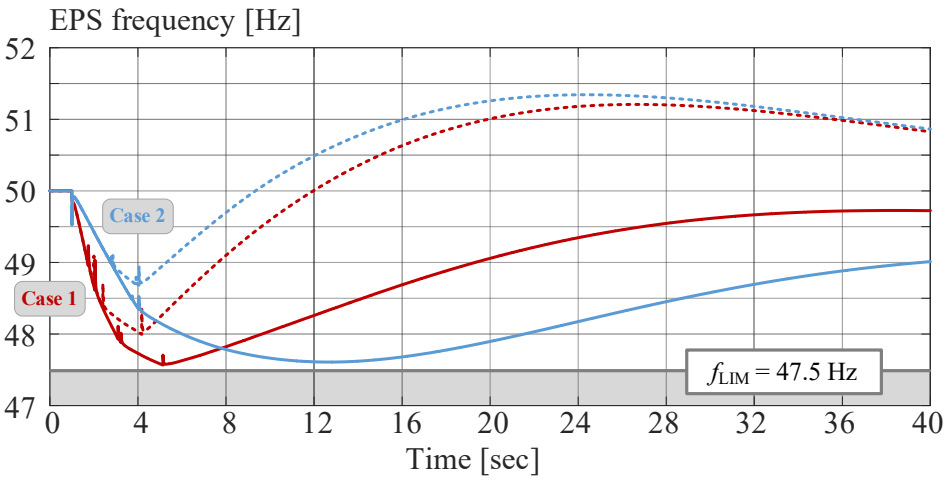

Fig. 6: Two out of 180 RMS dynamic simulation cases, showing the improvements in EPS frequency response when adding a new *RoCoF*-based tripping criterion

3.2 Real-time hardware-in-the-loop EMT dynamic simulations

The second most arguable concern that arises from the use of *RoCoF* is related to its noise level and numerical problems after events that affect power balance in the system (initial incident or UFLS activations) take place. For this purpose we proposed a special *RoCoF* filtering technique in [18], which involves sliding average filters and median filters. By implementing this filtering into a physical IED and including it in the HIL setup, we were able to obtain extremely well defined trajectories in the *f*-*M* plane that do not suffer from drawbacks usually attributed to *RoCoF*-supported algorithms. In Fig. 7, we plot an example from which it should be clear that since electro-mechanically driven *RoCoF* oscillations are well present in the *f*-*M* trajectory, the rest of the noise is effectively cancelled out. At this point it is important to stress that HIL RTDS simulations were performed for *RoCoF* values of up to -10 Hz/sec and we did not detect any undesired relay behaviour, nor did a new criterion cause any unplanned time delays. This is why we consider conditioning the tripping signal with a real-time frequency-stability margin value as a very effective and robust supplement to conventional UFLS setting.

4 Conclusions

In this paper, the very basics of a patent-pending solution of implementing locally measured *RoCoF* to frequency relays performing an UFLS task are presented alongside the latest relevant findings. Both the RMS as well as EMT dynamic simulations in terms of HIL testing proved the practical feasibility of adding an additional criterion to each frequency relay performing UFLS functionality. So we consider the technology to be at technology readiness level 5 (technology validated in lab) according to European Union scale. We indicated several positive outcomes of this UFLS enhancement, among which we have to stress an improved frequency response of the electrical power system under various operating conditions. The tests involved wide range of power-imbalance values as well as different inertia levels. The next stage of development will be oriented towards pilot installations to confirm the concept in the relevant environment (i.e. actual power system).

We detected several possibilities for further conceptual development as well. At this point we will list only three. First one is our primary focus and deals with setting up the procedures for frequency thresholds conditioning by the frequency-stability margin. Second, we are investigating how battery energy storage systems and CIG units

can benefit from locally calculated frequency-stability margin. The third is to analyse the possibilities to re-locate the load disconnections from a medium voltage level towards the end consumer that would enable one to decrease system loading without losing precious power generated by the distributed generating units.

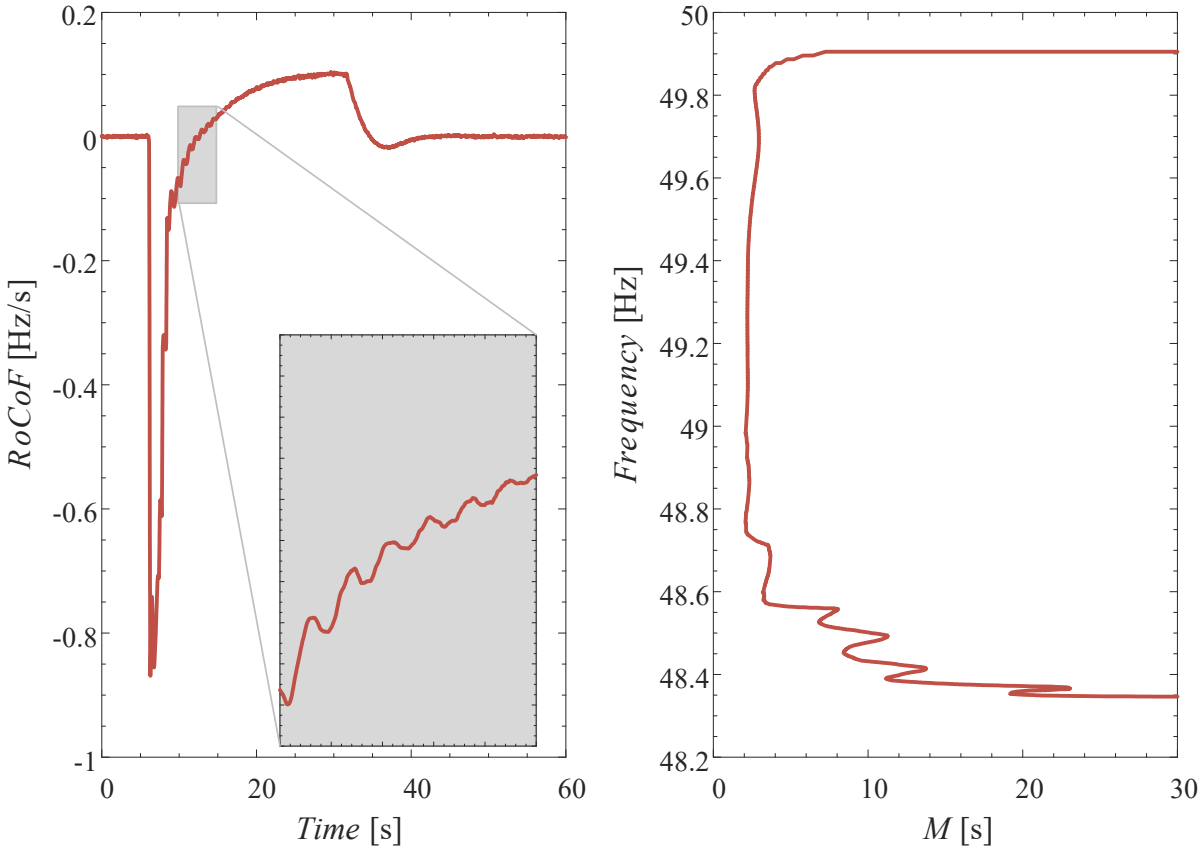

Fig. 7: Left: *RoCoF*(*t*) after an active-power incident as seen by the IED in HIL setup, right: corresponding trajectory in the *f*-*M* plane

5 References

[1] National Grid, 'Technical report on the events of 9 August 2019', Sep. 2019.

[2] ENTSO-E, 'System separation in the Continental Europe Synchronous Area on 8 January 2021 – 2nd update'. https://www.entsoe.eu/news/2021/01/26/system-separation-in-the-continental-europe-synchronous-area-on-8-january-2021-2nd-update/ (accessed Feb. 05, 2021).

[3] A. F.-P. in Islamabad, 'Nationwide power blackout plunges Pakistan into darkness', *the Guardian*, Jan. 10, 2021. http://www.theguardian.com/world/2021/jan/10/pakistan-power-gradually-being-restored-after-nationwide-blackout (accessed Jul. 02, 2021).

[4] E. Dehghanpour, H. K. Karegar, and R. Kheirollahi, 'Under Frequency Load Shedding in Inverter Based Microgrids by Using Droop Characteristic', *IEEE Trans. Power Deliv.*, vol. 36, no. 2, pp. 1097–1106, Apr. 2021, doi: 10.1109/TPWRD.2020.3002238.

[5] ENTSO-E, 'Research, Development & Innovation Roadmap 2020–2030'. Oct. 14, 2020. [Online]. Available: https://eepublicdownloads.entsoe.eu/clean-documents/Publications/RDC%20publications/entso-e-rdi_roadmap-2020-2030.pdf

[6] 'RG CE OH – Policy 5: Emergency Operations V 3.1'. ENTSO-E, Sep. 2017. [Online]. Available: https://docstore.entsoe.eu/Documents/Publications/SOC/Continental_Europe/oh/170926_Policy_5_ver3_1_43_RGCE_Plenary_approved.pdf

[7] ENTSO-E, 'Continental Europe Operation Handbook, Appendix 1: Load-Frequency Control and Performance'. Accessed: Feb. 23, 2015. [Online]. Available: https://www.entsoe.eu/publications/system-operations-reports/operation-handbook/Pages/default.aspx

[8] Md. A. Kabir, A. H. Chowdhury, and N.-A.- Masood, 'A dynamic-adaptive load shedding methodology to improve frequency resilience of power systems', *Int. J. Electr. Power Energy Syst.*, vol. 122, p. 106169, Nov. 2020, doi: 10.1016/j.ijepes.2020.106169.

[9] A. Chandra and A. K. Pradhan, ‘An Adaptive Underfrequency Load Shedding Scheme in the Presence of Solar Photovoltaic Plants’, *IEEE Syst. J.*, vol. 15, no. 1, pp. 1235–1244, Mar. 2021, doi: 10.1109/JSYST.2020.2995050.
[10] U. Rudez and R. Mihalic, ‘A novel approach to underfrequency load shedding’, *Electr. Power Syst. Res.*, vol. 81, no. 2, pp. 636–643, Feb. 2011, doi: 10.1016/j.epsr.2010.10.020.
[11] ‘IEEE Standard for Synchrophasor Measurements for Power Systems’, *IEEE Std C371181-2011 Revis. IEEE Std C37118-2005*, pp. 1–61, Dec. 2011, doi: 10.1109/IEEESTD.2011.6111219.
[12] ‘IEEE Standard for Synchrophasor Data Transfer for Power Systems’, *IEEE Std C371182-2011 Revis. IEEE Std C37118-2005*, pp. 1–53, Dec. 2011, doi: 10.1109/IEEESTD.2011.6111222.
[13] U. Rudez and R. Mihalic, ‘WAMS-Based Underfrequency Load Shedding With Short-Term Frequency Prediction’, *IEEE Trans. Power Deliv.*, vol. 31, no. 4, pp. 1912–1920, Aug. 2016, doi: 10.1109/TPWRD.2015.2503734.
[14] U. Rudez and R. Mihalic, ‘Predictive underfrequency load shedding scheme for islanded power systems with renewable generation’, *Electr. Power Syst. Res.*, vol. 126, pp. 21–28, Sep. 2015, doi: 10.1016/j.epsr.2015.04.017.
[15] U. Rudez and R. Mihalic, ‘RoCoF-based Improvement of Conventional Under-Frequency Load Shedding’, in *2019 IEEE Milan PowerTech*, Jun. 2019, pp. 1–5. doi: 10.1109/PTC.2019.8810438.
[16] ‘IEC 60255-181:2019 | IEC Webstore’. https://webstore.iec.ch/publication/30962 (accessed Jun. 09, 2020).
[17] R. Urban, S. Denis, and M. Rafael, ‘Estimating frequency stability margin for flexible under-frequency relay operation’, *Electr. Power Syst. Res.*, vol. 194, p. 107116, May 2021, doi: 10.1016/j.epsr.2021.107116.
[18] D. Sodin, R. Ilievska, A. Čampa, M. Smolnikar, and U. Rudez, ‘Proving a Concept of Flexible Under-Frequency Load Shedding with Hardware-in-the-Loop Testing’, *Energies*, vol. 13, no. 14, Art. no. 14, Jan. 2020, doi: 10.3390/en13143607.